2014 47th Hawaii International Conference on System Science

Phasor Measurement Unit Placement for Identifying Power Line Outages in Wide-Area Transmission System Monitoring

Hao Zhu
Dept of Electrical and
Computer Engineering
University of Illinois
Urbana, IL 61801-2918
Email: haozhu@illinois.edu

Yiyu Shi
Dept of Electrical and
Computer Engineering
Missouri Univ. of Science & Tech.
Rolla, MO 65409-0040
Email: yshi@mst.edu

Abstract

Phasor measurement units (PMUs) are widely recognized to be instrumental for enhancing the power system situational awareness – a key step toward the future power grid. With limited PMU resources and high installation costs, it is of great importance to develop strategic PMU deployment methods. This paper focuses on optimally selecting PMU locations for monitoring transmission line status across the wide-area grid. To bypass the combinatorial search involved, a linear programming reformulation is first developed to provide an upper bound estimate for the global optimum. Furthermore, a greedy heuristic method is adopted with the complexity only linearly in the number of PMUs, while leveraging on the upper bound estimate a branch-and-bound algorithm is also developed to achieve a near-optimal performance at a reduced complexity. Numerical tests on various IEEE test cases demonstrate the validity of our proposed methods, greatly advocating the satisfactory performance the simple greedy method at only linear complexity. This suggests a hybrid method by using the greedy solution as a warm start to reduce the number of BB iterations.

1. Introduction

The lack of comprehensive situational awareness in wide-area transmission systems has been identified as one of the key causes for major blackouts [21]. To build an accurate power system model in real time, it is highly crucial to timely monitor the status of generators, transformers, and transmission lines by collecting measurements from remote meters. Recently, phasor measurement units (PMUs) have been greatly advocated to enhance the power system situational awareness, due to their improved precision and higher sampling rate of measuring phasor angles [14].

Thanks to the enhanced sensing capability, the PMU devices have been exploited in a gamut of power system monitoring tasks, ranging from line outage identification [17], [18], [26] to state estimation [10], [12], to name a few. The tutorial paper [19] also provides a list of PMU-enabled applications. Notwithstanding the promising advancements that can be offered, the PMU penetration has so far been rather low, mainly limited by the associated installation and networking costs. According to the North American Synchrophasor Initiative (NASPI), the number of PMUs installed and networked in the easter/western interconnection is expected to in the order of 500 by the year 2014; see e.g. [10]. Hence, it is particularly critical for power system operators to judiciously select placement locations in view of the limited number of PMU devices.

Several works have addressed how to optimally place PMUs to support power system state estimation [10], [12]. A max-min error norm criterion has been proposed in [24] for line outage identification purpose. There also exists a large volume of literature on the PMU placement strategies for topological observability; see e.g., [10], [12] and references therein. Even though the full range of PMU-enabled applications has not yet been fully understood, it is widely appreciated that the PMU placement problem needs to be addressed under a task-specific framework.

The present paper is focused on the task of identifying power *line outages* using the wide-area voltage *phasor angle measurements* provided by PMUs in real time. Relying on the grid-wide *basecase* information from the NERC System Data Exchange (SDX) module [22], it has been demonstrated in [17], [18], [26] that the grid topology change is detectable using only *a subset of* phase angle measurements, even for the case of multiple line outages. To exactly improve the identification performance, the present work proposes to find the optimal PMU locations by maximizing the success rate of correctly detecting the line-outage events. It is worthy pointing out that the line-outage identification framework developed here can be extended to monitor more general power system disturbances such as generator outages and load changes. Hence, the proposed algorithms would also be instructive for optimally placing PMUs to enhance the model observability in validating generator or load parameters, and even broadly for system anomaly detections.

The PMU placement problem for line outage identification can be explicitly formulated as a discrete set optimization problem (Section 2), for which finding the global optimum is likely to incur a combinatorial complexity. To make it

978-1-4799-2504-9/14 $31.00 © 2014 IEEE
DOI 10.1109/HICSS.2014.311

more tractable, a linear programming (LP) reformulation is introduced by relaxing the combinatorial constraint as well as advocating an approximation of the objective function (Section 3). However, it turns out the LP reformulation can only attain a loose upper bound for the original PMU placement problem. To directly tackle the combinatorial constraint, a greedy heuristic method is adopted with only linear complexity in the number of PMU devices, while a branch-and-bound algorithm has also been offered which can attain a near-optimal solution (Section 4). Simulated tests corroborate the merits of the proposed algorithms and illustrate the trade-off between performance and complexity (Section 5). The simplified assumptions used are discussions and the proposed algorithms are extended to more general scenarios (Section 6). The paper is wrapped up with a concluding summary (Section 7).

Notation: Upper (lower) boldface letters will be used for matrices (column vectors); $(\cdot)^T$ denotes transposition; $(\cdot)^{-1}$ the matrix inverse; diag$(\ldots)$ the diagonalization operator; $\odot$ the entry-wise dot-product operator; $\mathbf{1}$ the all-one vector; $\mathbf{0}$ the all-zero vector; $\|\cdot\|_p$ the vector $p-$norm for $p \geq 1$; $|\cdot|$ the magnitude or cardinality of a set; $\mathcal{S}_1 \backslash \mathcal{S}_2$ the relative complement of the set $\mathcal{S}_2$ in the set $\mathcal{S}_1$.

2. PMU placement: A first look

This section provides the modeling basics for our work and the PMU placement problem formulation.

2.1. Models and assumptions

Consider a power transmission network with the reference bus 0, N buses in the set $\mathcal{N} := \{1, \ldots, N\}$, and L transmission lines in the set $\mathcal{E} := \{1, \ldots, L\}$. Collect the voltage phasor angles $\{\theta_n\}$ for all buses in $\mathcal{N}$, in the vector $\boldsymbol{\theta} \in \mathbb{R}^N$; and similarly for the injected real power $\{P_n\}$ in $\mathbf{p} \in \mathbb{R}^N$. The linearized DC power flow model is used only to motivate the sparse overcomplete formulation for the line outage identification problem. However, it is worthy pointing out that our placement method does not reply on the DC approximation at all, and in fact the AC flow model is assumed for developing the PMU placement method both analytically and numerically. This will become more clear later in Section 6.

The linearized DC power flow model asserts

$$\mathbf{p} = \mathbf{B}\boldsymbol{\theta}, \tag{1}$$

where $\mathbf{B}$ is the $N \times N$ bus susceptance matrix; see e.g., [23, Ch. 4]. Matrix $\mathbf{B}$ is uniquely determined by all line susceptance $\{b_\ell\}_{\ell=1}^L$, and the network topology $\mathcal{E}$. It has been shown in [26] that $\mathbf{B}$ can be viewed as the weighted Laplacian matrix for the graph $(\mathcal{N}, \mathcal{E})$. To this end, consider the $N \times L$ bus-line incidence matrix $\mathbf{M}$, where its ℓ-th column $\mathbf{m}_\ell$ has only two non-zero entries ± 1 corresponding to the two end-buses for line $\ell \in \mathcal{E}$. The weighted graph Laplacian is thus given by

$$\mathbf{B} = \sum_{\ell=1}^{L} b_\ell \mathbf{m}_\ell \mathbf{m}_\ell^T = \mathbf{M}\mathbf{D}_b\mathbf{M}^T \tag{2}$$

where $\mathbf{D}_b := \text{diag}(b_1, \ldots, b_L)$. Notice that $\mathbf{B}$ is of full rank and invertible after excluding the reference bus 0.

Suppose that due to changes in the system, e.g., cascading failures at an early stage, several outages occur at the lines in $\tilde{\mathcal{E}} \subseteq \mathcal{E}$. Line outages in the transmission network yield the post-event graph $(\mathcal{N}, \mathcal{E}')$, with[1] $\mathcal{E}' := \mathcal{E} \backslash \tilde{\mathcal{E}}$. As in [17], [18], [26], it is assumed that fast system dynamics are well damped, and that the system settles down to a quasi-stable state following the line outages. Furthermore, assume that the outage lines in $\tilde{\mathcal{E}}$ will not result in islanding of the post-event system; that is, the underlying graph will not become disconnected. This precludes considerable changes between pre- and post-event bus power injections, and the load profile variation becomes negligible under the timescale of outage events. Hence, the linear DC model for the quasi-stable post-event network yields [cf. (1)]

$$\mathbf{p} = \mathbf{B}'\boldsymbol{\theta}' \tag{3}$$

where $\mathbf{B}'$ is the corresponding post-event weighted Laplacian for $(\mathcal{N}, \mathcal{E}')$.

The weighted Laplacian representation immediately implies that the difference $\mathbf{B} - \mathbf{B}' = \sum_{\ell \in \tilde{\mathcal{E}}} b_\ell \mathbf{m}_\ell \mathbf{m}_\ell^T$. Substituting this and (3) into (1) leads to the following for the phase angle difference $\tilde{\boldsymbol{\theta}} := \boldsymbol{\theta}' - \boldsymbol{\theta}$

$$\mathbf{B}\tilde{\boldsymbol{\theta}} = (\mathbf{B} - \tilde{\mathbf{B}})\boldsymbol{\theta}' = \sum_{\ell \in \tilde{\mathcal{E}}} s_\ell \ \mathbf{m}_\ell \tag{4}$$

where $s_\ell := b_\ell \mathbf{m}_\ell^T \boldsymbol{\theta}$, $\forall \ell$. Upon defining $\mathbf{a}_\ell := \mathbf{B}^{-1}\mathbf{m}_\ell$, solving (4) with respect to (wrt) $\tilde{\boldsymbol{\theta}}$ yields

$$\tilde{\boldsymbol{\theta}} = \mathbf{B}^{-1}\left(\sum_{\ell \in \tilde{\mathcal{E}}} s_\ell \ \mathbf{m}_\ell\right) = \sum_{\ell \in \tilde{\mathcal{E}}} s_\ell \ \mathbf{a}_\ell. \tag{5}$$

This relation between $\tilde{\mathcal{E}}$ and $\tilde{\boldsymbol{\theta}}$ intuitively explains why it is possible to utilize synchrophasor data to identify line outages. Similar to the notion of line outage distribution factor (LODF) which reflects changes in the real power flow during power system contingencies [9], the vector $\mathbf{a}_\ell$ can be considered as the signature vector for the line ℓ, in terms of changes in the bus phasor angle.

2.2. Problem statement

This paper focuses on the problem of placing PMUs to maximize the performance for identifying line outages. Given the budget of N_P PMU devices, let $\mathcal{N}_P \subseteq \mathcal{N}$ denote the subset of N_P locations chosen for PMU installation. Accordingly, let $\boldsymbol{\theta}_P$ be the observable sub-vector of $\boldsymbol{\theta}$, collecting phasor angles

1. As a mnemonic, post-event quantities are denoted with prime, and the differences relative to their pre-event counterparts are denoted with tilde.

at buses in $\mathcal{N}_P$; and similarly for the sub-vectors $\boldsymbol{\theta}'_P$ and $\tilde{\boldsymbol{\theta}}_P$. Extracting only the rows in (4) corresponding to $\mathcal{N}_P$, one can obtain

$$\tilde{\boldsymbol{\theta}}_P = \sum_{\ell \in \tilde{\mathcal{E}}} s_\ell \ \mathbf{a}_{\ell,P} \tag{6}$$

where $\mathbf{a}_{\ell,P}$ is also constructed by selecting the entries from $\mathcal{N}_P$.

Now the problem amounts to identifying the lines in $\tilde{\mathcal{E}}$ using the available $\tilde{\boldsymbol{\theta}}_P$. By enumerating all the line combinations for a given cardinality of $\tilde{\mathcal{E}}$, it is possible to exhaustively check the least-squares (LS) error norm of reconstructing $\tilde{\boldsymbol{\theta}}$ for each candidate scenario, and select the one with the minimum cost; see e.g., [17], [18]. This enumerative search (ES) method incurs a combinatorial complexity that grows with the number of lines in $\tilde{\mathcal{E}}$. To tackle this, a fresh sparse overcomplete representation has been proposed in [26] for the system model (6), which allows to leverage exciting ideas from compressive sensing (CS) [5], [20] for identifying $\tilde{\mathcal{E}}$. Among various CS algorithms, the greedy orthogonal matching pursuit (OMP) approach [20] has been advocated by [26] as an efficient and (near-)optimal alternative to the ES. The OMP has been deemed as the algorithm to be able to cope with the real-time monitoring requirement for multiple line outages in practise. More interestingly, the OMP leads directly to a tractable characterization for the event of successful detection. Hence, it will be used as the identification method in the present paper.

To better characterize the objective, this paper will also consider only single line-outage events, namely, $|\tilde{\mathcal{E}}| = 1$. The reason is two-fold. First, as demonstrated by the numerical analysis in [26], the identification error rate for single line outages is extremely close to that of the double outages. Second, it can be shown that if the vectors $\{\mathbf{a}_{\ell,P}\}$ are nearly orthogonal, the coupling among lines is very weak and it is possible to decompose the multiple line outages to single cases. In the large-scale power systems, the coupling of lines should be very weak for us to focus on only single line outages. Hence, this simplification can be deemed very representative of the overall system performance even with multiple line outages.

Given a single line-outage event $\tilde{\mathcal{E}} = \{\ell\}$, let the vector $\mathbf{y}_{\ell,P} \in \mathbb{R}^{N_P \times 1}$ denote the copy of $\tilde{\boldsymbol{\theta}}$ obtained numerically through contingency analysis using the *AC power flow model*. In practical power systems, the measurement $\mathbf{y}_{\ell,P}$ would account for system uncertainties due to the operating point and metering noise. The noise can be assumed negligible for the high-rate and synchronous PMU data, whereas the system operating point may vary vastly depending on different load profiles. For simplicity, this majority of the paper will focus on one basic load profile case. Extensions to account for multiple operating points are possible, as detailed in Section 6. The assumptions on single line outages as well as the OMP will also be discussed then.

Assuming all signature vectors $\{\mathbf{a}_\ell\}$ have been normalized to be of unit Euclidean norm, the OMP method would identify the outage line as

$$\hat{\ell} := \arg\max_{k \in \mathcal{E}} |\mathbf{y}_{\ell,P}^T \ \mathbf{a}_{k,P}|. \tag{7}$$

Without loss of generality (Wlog), the sign of $\mathbf{y}_\ell$ can be flipped to make sure that $\mathbf{y}_{\ell,P}^T \mathbf{a}_{\ell,P} \geq 0$ always holds. Hence, the outaged line ℓ is correctly identified if and only if (iff)

$$\mathbf{y}_{\ell,P}^T \mathbf{a}_{\ell,P} \geq |\mathbf{y}_{\ell,P}^T \mathbf{a}_{k,P}|, \quad \forall k \in \mathcal{E}. \tag{8}$$

A weighting coefficient $\alpha_\ell \in [0,1]$ is introduced here that associates with any line ℓ. The value α_ℓ is chosen depending on the impact if the system operator can correctly detect the outage event occurring at line ℓ. One simple choice is the uniform weighting rule where $\alpha_\ell = (1/L)$, $\forall \ell \in \mathcal{E}$. However, in practical power systems, some transmission lines such as those high-voltage ones could carry much larger power flows, and thus they are of higher priority for the control center to monitor. To account for this, it is possible to choose α_ℓ to be proportional to the pre-event real power flow on line ℓ. With $\{\alpha_\ell\}$ given, the weighted success rate of identifying all single line-outage events is given for any subset $\mathcal{N}_P$, as

$$f(\mathcal{N}_P) := \sum_{\ell \in \mathcal{E}} \alpha_\ell \mathbb{1}\{\mathbf{y}_{\ell,P}^T \mathbf{a}_{\ell,P} \geq |\mathbf{y}_{\ell,P}^T \mathbf{a}_{k,P}|, \ \forall k \in \mathcal{E}\} \tag{9}$$

where the indication function $\mathbb{1}(\cdot) = 1$ if the statement is true, otherwise 0. Given the budget of N_P PMU devices, the problem of interest becomes how to select the locations to maximize the weighted success rate, as given by

$$\begin{aligned} f^\star := \max_{\mathcal{N}_P \subseteq \mathcal{N}} \quad & f(\mathcal{N}_P) \\ \text{s. t.} \quad & |\mathcal{N}_P| \leq N_P. \end{aligned} \tag{10}$$

The PMU placement problem (10) is complicated by two issues. First, the optimization variable $\mathcal{N}_P$ is a discrete subset, which implies a combinatorial problem complexity in the number of candidate bus locations. Second, the presence of the indicator function makes it more difficult in terms of evaluating the objective cost, as elaborated soon. As will be shown in the ensuing section, the problem (10) can be reformulated as a non-convex Mixed-Integer NonLinear Program (MINLP), and thus is generally NP-hard; see e.g., [4]. This motivates us to first approximate the objective cost to a concave function, and further relax it to a linear program.

3. A linear programming reformulation

This section will offer a reformulation of the PMU placement problem (10), using an approximate objective function and the convex relaxation technique. This reformulation not only provides a coarse approximate solution to the original problem, but also turns out to be useful for developing a more sophisticated algorithm later.

To simplify (9), define the $N \times 1$ vector $\mathbf{c}_{\ell k} := \mathbf{y}_\ell \odot \mathbf{a}_k$ as the dot product vector for any $k, \ell \in \mathcal{E}$, and an $N \times 1$ indicator vector $\mathbf{w}_P \in \{0,1\}^N$ corresponding to $\mathcal{N}_P$ such that

$$w_{n,P} := \begin{cases} 1, & \text{if } n \in \mathcal{N}_P, \\ 0, & \text{otherwise.} \end{cases} \tag{11}$$

Clearly, any subset $\mathcal{N}_P \subseteq \mathcal{N}$ can be uniquely represented by a vector $\mathbf{w}_P \in \{0,1\}^N$; and also the other way around. With these notations, the event of correctly identifying line ℓ in (9) now yields

$$\begin{aligned} & \mathbb{1}\left\{\mathbf{w}_P^T\mathbf{c}_{\ell\ell} \geq |\mathbf{w}_P^T\mathbf{c}_{\ell k}|,\ \forall k\right\} \\ = \ & \mathbb{1}\left\{\mathbf{w}_P^T\mathbf{c}_{\ell\ell} - \mathbf{w}_P^T\mathbf{c}_{\ell k} \geq 0, \mathbf{w}_P^T\mathbf{c}_{\ell\ell} + \mathbf{w}_P^T\mathbf{c}_{\ell k} \geq 0, \forall k\right\} \end{aligned}$$

which is equivalent to having the minimum of all these difference terms to be non-negative. Recalling the one-to-one correspondence between $\mathcal{N}_P \subseteq \mathcal{N}$ and $\mathbf{w}_P \in \{0,1\}^N$, the identification success rate in (9) can take $\mathbf{w}_P$ as its variable, as

$$f(\mathbf{w}_p) := \sum_{\ell\in\mathcal{E}} \alpha_\ell \mathbb{1}\Big\{\min_k \left\{\mathbf{w}_P^T(\mathbf{c}_{\ell\ell} - \mathbf{c}_{\ell k}),\right. \\ \left. \mathbf{w}_P^T(\mathbf{c}_{\ell\ell} + \mathbf{c}_{\ell k})\right\} \geq 0\Big\}. \quad (12)$$

The PMU placement problem in (10) can be cast as one over an $N \times 1$ vector $\mathbf{w}$, as given by

$$\begin{aligned} f^\star = \max_{\mathbf{w},\{t_\ell\}} \quad & \sum_{\ell\in\mathcal{E}} \alpha_\ell \mathbb{1}\{t_\ell \geq 0\} \\ \text{s. t.} \quad & t_\ell \leq \mathbf{w}^T(\mathbf{c}_{\ell\ell} - \mathbf{c}_{\ell k}),\ \forall k,\ell \\ & t_\ell \leq \mathbf{w}^T(\mathbf{c}_{\ell\ell} + \mathbf{c}_{\ell k}),\ \forall k,\ell \\ & \sum_{n\in\mathcal{N}} w_n \leq N_P \\ & w_n \in \{0,1\},\quad \forall n \in \mathcal{N} \end{aligned} \quad (13)$$

where the auxiliary variable t_ℓ is introduced to represent the minimum of all the difference terms per line ℓ. Compared to the discrete set optimization in (10), the reformulation in (13) is more tractable. For example, its first three constraints are all linear, and thus convex over $\mathbf{w}$ and t_ℓ. However, the indicator operator $\mathbb{1}(\cdot)$ actually yields the unit step function as shown in Fig. 1, hence the objective in (13) is not concave over t_ℓ. Thus, this equivalent formulation (13) still gives rise to a non-convex problem in addition to its binary constraints. This implies that even its *continuous relaxation* by relaxing the binary alphabet to the interval constraint is likely to be NP-hard or eve nundecidable; see e.g., [4] and the references therein. This speaks for how intractable the non-convex MINLP problem (13) could be.

To tackle this, we propose to relax (13) to a convex linear program. The continuous relaxation is performed using the interval constraint $0 \leq w_n \leq 1, \forall n$ [3]. There also exist other more sophisticated convex relaxation methods, such as the semidefinite relaxation (SDR) technique that would lead to a semidefinite program; see e.g., [8]. In this work, we choose the interval relaxation for its simplicity. To tackle the non-concave cost function, we propose to replace the operator $\mathbb{1}\{t_\ell \geq 0\}$ of the objective in (13) using the following approximation as shown in Fig. 1

$$g(t_\ell) := \min\{1, 1 + t/c\} \quad (14)$$

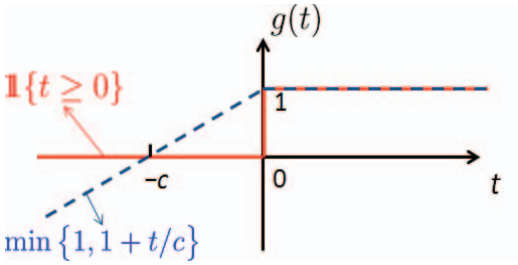

Fig. 1. The unit step function (in solid line) and its approximate function $g(\cdot)$ (in dashed line).

for some $c > 0$. Since $g(\cdot)$ is the minimum of two concave functions, itself is also concave.

As elaborated later, it will be useful to find an upper bound estimate for the optimal value of the original problem (13). Therefore, the positive c needs to be chosen to make sure that $g(t_\ell) > 0$ always holds; i.e., $t_\ell \geq -c$ for any $\ell \in \mathcal{E}$. Recalling that t_ℓ is the minimum of all the difference terms in (12), and also noting that no entry of $\mathbf{w}$ would exceed N_P, one can select

$$c = N_p \times \min\{c^-, c^+\} \quad (15)$$

where c^- is the minimum entry among all the vectors $\{\mathbf{c}_{\ell\ell} - \mathbf{c}_{\ell k}\}_{\ell,k}$, and c^+ the minimum entry among all $\{\mathbf{c}_{\ell\ell} + \mathbf{c}_{\ell k}\}_{\ell,k}$.

Under this setting, it is guaranteed that $g(t_\ell) \geq \mathbb{1}\{t_\ell \geq 0\}$ over the region of interest. Furthermore, the convex interval relaxation would expand the feasibility set for the maximization problem. Hence, it is possible to attain an upper bound for the maximum of (13) by solving

$$\begin{aligned} \max_{\mathbf{w},\{t_\ell,g_\ell\}} \quad & \sum_{\ell\in\mathcal{E}} \alpha_\ell g_\ell \\ \text{s. t.} \quad & g_\ell \leq 1,\ g_\ell \leq 1 + t_\ell/c,\ \forall \ell \\ & t_\ell \leq \mathbf{w}^T(\mathbf{c}_{\ell\ell} - \mathbf{c}_{\ell k}),\ \forall k,\ell \\ & t_\ell \leq \mathbf{w}^T(\mathbf{c}_{\ell\ell} + \mathbf{c}_{\ell k}),\ \forall k,\ell \\ & \sum_{n\in\mathcal{N}} w_n \leq N_P \\ & 0 \leq w_n \leq 1,\quad \forall n \in \mathcal{N} \end{aligned} \quad (16)$$

where the auxiliary variable g_ℓ would be equal to the value $g(t_\ell)$ at the optimum. The reformulated problem (16) is actually a linear program (LP); see e.g., [3]. The computational complexity for LP problems is typically polynomial in the problem dimension, which grows quadratically with the number of lines as in (16). There are some efficient solvers to find the global optimum, such as the interior-point method [16]. Upon obtaining the optimum to (16), the achieved maximal cost can be considered as the upper bound for the optimal cost of (13). Furthermore, although the solution of (16) is no longer binary due to the relaxation, it is still possible to find an approximate solution to the original problem (13) by setting its largest N_P entries to 1, and zero the rest [3]. This approximate

solution would attain a lower bound for the original optimal cost of (13).

The LP formulation in (16) is not only efficiently solvable, but also provides some bounding results for the optimal values of (13). Nonetheless, the numerical tests will illustrate that these bounds could be very loose. In lieu of this approach, the ensuing section will propose two (sub-)optimal algorithms to directly tackle the binary constraint of (13).

4. (Sub-)optimal algorithms

One of the major limitations of the proposed LP formulation is that it fails to respect the binary constraint in (13) . Next, two (sub-)optimal PMU placement algorithms are developed to account for such constraint explicitly.

4.1. A greedy heuristic method

The greedy method is first adopted for the PMU placement problem (10), as tabulated in Algorithm 1. This heuristic approach is initialized with a pre-selected subset of buses $\mathcal{N}_P^o$, such as the empty set $\emptyset$ if no bus has been selected so far. It proceeds by iteratively choosing the next PMU bus location that achieves the largest 'marginal' cost in terms of (9), one bus at a time until the solution $\mathcal{N}_P^{\mathrm{G}}$ reaches the cardinality budget N_P. Notice that although Algorithm 1 adopts the set/element notations, it can be easily represented using the indicator vector $\mathbf{w}$ as well.

Clearly, the complexity of such iterative scheme grows only linearly with the number of available PMU devices, which makes it extremely suitable for implementation in large-scale systems. In addition to the low complexity, the buses selected at an early stage are always maintained even if the budget N_P increases later on, which is termed as the *consistency property* for the solutions of the greedy method. This nested property also makes it a very attractive scheme for PMU placement in general, since it can easily accommodate any future system expansion plans if more and more PMU devices become available. For this reason, the greedy method has been very popular in several other PMU placement works for e.g., improving the power system state estimation in [12], and optimizing the max-min error criterion in [24].

Remark 1. *(Greedy's performance.)* Although the greedy method seems to be simply heuristic, it is provable to achieve an approximation ratio of $(1 - 1/e)$ to the optimum for some specific discrete set optimization problems, as in [12]. This performance guarantee can be established if the problem objective function is shown to satisfy the so-termed 'sub-modularity' property; see e.g., [13]. In general, the objective function does not need to be strictly submodular as long as it can be approximated as a submodular one under some conditions [7]. It is very promising to show that the detection success rate function (9) is approximately submodular based on the increasing curves in the numerical results. This helps explain why the greedy solution achieves the near-optimal performance numerically. Future research directions open up to investigate its performance guarantee by possibly showing that the objective (9) is approximately submodular.

Algorithm 1 (Greedy): Input N_P, $\{\mathbf{y}_\ell\}$, $\{\mathbf{a}_\ell\}$, and the initial set $\mathcal{N}_P^o$. Output $\mathcal{N}_P^{\mathrm{G}} = \mathcal{N}_P^o \cup \{n_\rho\}_{\rho=1}^{N_P - |\mathcal{N}_P^o|}$.

Initialize $\mathcal{N}_P^{\mathrm{G}} \leftarrow \mathcal{N}_P^o$, and compute all the dot-product vectors $\mathbf{c}_{\ell k} = \mathbf{y}_\ell^T \mathbf{a}_k$, for any $k, \ell \in \mathcal{E}$.

for $\rho = 1, \ldots, N_P - |\mathcal{N}_P^o|$ **do**

Find $n_\rho = \arg\max_{n \notin \mathcal{N}_P^{\mathrm{G}}} f(\mathcal{N}_P^{\mathrm{G}} \cup \{n\})$;

Update $\mathcal{N}_P^{\mathrm{G}} \leftarrow \mathcal{N}_P^{\mathrm{G}} \cup \{n_\rho\}$.

end for

4.2. A branch-and-bound algorithm

To improve the gap between the greedy and the optimal solutions, we develop a branch-and-bound (BB) algorithm [2], [11] to solve for (13). It can obtain a feasible and δ-optimum solution $\mathbf{w}^\star$ satisfying: a) $w_n^\star \in \{0, 1\}$ and $\sum_{n \in \mathcal{N}} w_n^\star \leq N_P$; and b) $f^\star \leq f(\mathbf{w}^\star) \leq f^\star + \delta$, where δ denotes a pre-specified margin and $f^\star$ is the optimum value for (13). Although by relaxing the objective, it is possible to cast (13) as a mixed-integer linear program (MILP) and use generic BB-based solvers for it, the *continuous relaxation* would lead to very bad approximation results. This motivates us to specifically develop a BB method for (13) which accounts for the non-concave cost function.

The BB algorithm successively improves the estimates of *lower and upper bounds* on the optimum $f^\star$ of (13), by splitting one candidate solution into two cases. Let i be the iteration index, and L_i and U_i stand for the lower and upper bounds per iteration i, respectively. At iteration $i = 1$, Algorithm 1 can be invoked with $\mathcal{N}_P^o = \emptyset$ to provide an initial lower bound, as given by $L_1 = f(\mathcal{N}_P^{\mathrm{G}})$. The optimal value of (16) can also be obtained efficiently as the initial upper bound U_1. To proceed to iteration $i = 2$, pick one bus $\nu \in \mathcal{N}$ to split the problem (13) into two sub-problems by fixing w_ν to be either 0 or 1, as given by

$$\begin{aligned} \max_{\mathbf{w}, \{t_\ell\}} \quad & \sum_{\ell \in \mathcal{E}} \alpha_\ell \mathbb{1}\{t_\ell \geq 0\} \\ \text{s. t.} \quad & t_\ell \leq \mathbf{w}^T(\mathbf{c}_{\ell\ell} - \mathbf{c}_{\ell k}),\ \forall k, \ell \\ & t_\ell \leq \mathbf{w}^T(\mathbf{c}_{\ell\ell} + \mathbf{c}_{\ell k}),\ \forall k, \ell \\ & \sum_{n \in \mathcal{N}} w_n \leq N_P,\ w_\nu = 0 \\ & w_n \in \{0, 1\},\quad \forall n \neq \nu \end{aligned} \tag{17}$$

and

$$\begin{aligned}\max_{\mathbf{w},\{t_\ell\}} \quad & \sum_{\ell\in\mathcal{E}} \alpha_\ell \mathbb{1}\{t_\ell \geq 0\} \\ \text{s. t.} \quad & t_\ell \leq \mathbf{w}^T(\mathbf{c}_{\ell\ell} - \mathbf{c}_{\ell k}),\ \forall k,\ell \\ & t_\ell \leq \mathbf{w}^T(\mathbf{c}_{\ell\ell} + \mathbf{c}_{\ell k}),\ \forall k,\ell \\ & \sum_{n\in\mathcal{N}} w_n \leq N_P,\ w_\nu = 1 \\ & w_n \in \{0,1\},\quad \forall n \neq \nu. \end{aligned} \tag{18}$$

To find the upper bounds $u_2^{(0)}$ and $u_2^{(1)}$ for sub-problems (17) and (18), respectively, similar techniques as in (16) can be used to reformulate them to LP problems. It is possible to obtain their respective lower bounds $l_2^{(0)}$ and $l_2^{(1)}$ using the greedy heuristic method. Notice that Algorithm 1 needs to be slightly modified to account for the constraint $w_\nu = 0$ in (17) by muting bus ν from the selection pool, while $l_2^{(1)}$ can simply obtained by initializing $\mathcal{N}_P^o = \{\nu\}$. Upon solving for these bounds, the lower and upper bounds are further refined as

$$\begin{aligned} L_2 &= \max\{l_2^{(0)}, l_2^{(1)}\}, \\ \text{and } U_2 &= \max\{u_2^{(0)}, u_2^{(1)}\}. \end{aligned} \tag{19}$$

Such splitting process corresponds to the branch part of the BB algorithm to generate a pair of candidate solutions from an existing one. Per iteration i, L_i and U_i are always updated as the maximum lower and upper bounds achieved so far.

To eventually bound the estimates of $f^\star$, the BB algorithm also keeps the list of candidate solutions $\mathcal{S}$. Once a new candidate solution is generated by the splitting process, it will be augmented to the list $\mathcal{S}$ if and only if its upper bound exceeds the current L_i. Otherwise, this candidate solution will definitely not be the global optimum and thus can be trimmed from any future considerations.

The detailed BB scheme is tabulated in Algorithm 2. To computer the lower and upper bounds, $LB(\cdot)$ and $UB(\cdot)$ denote the aforementioned methods based on either the greedy heuristic or the LP reformulation. Algorithm 2 always picks the candidate with the largest upper bound to split, and splits at the first bus with the best marginal improvement as suggested by Algorithm 1. If only one bus is needed in $\bar{\mathbf{w}}$ ($\sum_n \bar{w}_n = N_P - 1$), that first bus can be added to find the actual best cost under this scenario. Otherwise, a pair of candidate solutions are generated to improve the estimates for lower and upper bounds of $f^\star$. When the gap between the two diminishes to δ, the solution that achieves the best lower bound is guaranteed to be δ-optimal.

Remark 2. *(Computational complexity.)* Albeit near-optimal, the BB algorithm may exhibit the combinatorial complexity in the worst case. In general its computational complexity is very difficult to characterize. Numerical tests also show that the runtime for the BB algorithm could be intractable for large systems. Fortunately, the runtime for the BB method can be greatly reduced by using parallel computing resources, which is beyond the scope of this paper. Interested readers are referred to [1], [6] for more details. It is also possible to limit the runntime by setting a budget on the total number of iterations in practice.

Algorithm 2 (BB): Input N_P, $\{\mathbf{y}_\ell\}$, $\{\mathbf{a}_\ell\}$, and the threshold δ. Output a δ-optimal solution $\mathbf{w}^\star$ of (13).

Set $i = 1$, and compute all the dot-product vectors $\mathbf{c}_{\ell k} = \mathbf{y}_\ell^T \mathbf{a}_k$, for any $k, \ell \in \mathcal{E}$.

Set $\mathbf{w} = \mathbf{0}$, and compute $L_1 = LB(\mathbf{w})$ as well as $U_1 = UB(\mathbf{w})$.

Initialize $\mathcal{S} \leftarrow \{(\mathbf{w}, L_1, U_1)\}$.

while $U_i - L_i \geq \delta$ {need to split} **do**

Let $(\bar{\mathbf{w}}, \bar{L}, \bar{U})$ be one triplet of $\mathcal{S}$ with the largest upper bound and $\sum_n \bar{w}_n < N_P$; and set $\mathcal{S} = \mathcal{S}\backslash(\bar{\mathbf{w}}, \bar{L}, \bar{U})$.

if $\sum_n \bar{w}_n = N_P - 1$ {only one more bus needed} **then**

Use Algorithm 1 to find the best bus location n_1, and set $\bar{w}_{n_1} = 1$.

Compute $l = LB(\bar{\mathbf{w}})$, and augment the list $\mathcal{S} \leftarrow \mathcal{S} \cup \{(\bar{\mathbf{w}}, l, l)\}$.

else

Use Algorithm 1 to find the first bus ν to split.

Form the pair of candidate solutions $\mathbf{w}^{(0)}$ and $\mathbf{w}^{(1)}$ from splitting on bus ν of $\bar{\mathbf{w}}$, e.g., $w_\nu^{(0)} = 0$ and $w_\nu^{(1)} = 1$.

Compute their respective upper (lower) bounds $u^{(0)}$ and $u^{(1)}$ ($l^{(0)}$ and $l^{(1)}$).

Augment the list $\mathcal{S} = \mathcal{S} \cup \{(\mathbf{w}^{(k)}, l^{(k)}, u^{(k)}\}$ for $k \in \{0,1\}$ only if $u^{(k)} \geq L_i$.

end if

Update $i \leftarrow i + 1$, and the bounds L_i and U_i to be the respective maxima of all the triplets in $\mathcal{S}$.

end while

Let $(\mathbf{w}^\star, L^\star, U^\star)$ with the largest lower bound in $\mathcal{S}$, and update $\mathbf{w}^\star$ as the greedy solution with N_P total PMU devices.

5. Numerical examples

This section simulates the proposed PMU placement algorithms numerically using several IEEE benchmark test systems in [15]. The software toolbox MATPOWER [25] is used throughout to generate the pertinent AC power flows under one basic load profile, as well as the pertinent phasor angle data $\mathbf{y}_\ell$ for every $\ell \in \mathcal{E}$. It is worthy pointing out that since the simulated tests are generated based on the AC power flow model, the experimental results here reflect the performance for the actual power systems. The reference bus is assumed to be equipped with the PMU for providing the relative angel reference, and thus it is not included in $\mathcal{N}$. All the three algorithms presented in this paper, namely the approximation based on LP, Algorithm 1 (Greedy), and Algorithm 2 (BB),

have been tested and compared.

All the three algorithms are first tested using the IEEE 14-bus, RTS 24-bus, and 30-bus systems. The LP approximation solution is rounded with an indicator vector by selecting its largest N_P entries to be 1. For the BB algorithm, the threshold δ is chosen to be small enough ($\sim 10^{-3}$) to yield the global optimum solution to (13). The weights α_ℓ are scaled to be proportional to the pre-event real power flow on line ℓ. Fig. 2 plots the weighted success rate in (12) versus the budget N_P.

As depicted in Fig. 2, the success rate attained by the LP approximation could be quite bad for some cases, especially if N_P is at the medium range (around $N/2$). This is expected since the LP formulation fails to account for the binary constraint of the original placement problem. Most interestingly, the greedy heuristic is extremely competitive as compared to the global optimum, almost identical for the 24-bus system. This is surprising since the greedy algorithm has a much more attractive computational complexity. The success rate function exhibits the shape of 'diminishing marginal return' property, thus it is very likely that it can be approximated to a submodular function. This would explain the near-optimal performance of the greedy heuristic method.

It is also observed that when N_P is small (less than $N/2$), the performance improvement with one additional PMU device is much higher compared to a larger N_P. Even with around half of buses equipped with PMUs ($N_P \sim N/2$), the line outage identification performance is very close to perfect at more than 80% of success rate. After that, additional PMU devices do not seem to benefit with much improvement in the performance. This again verifies the observations in existing works the best reward is attained with 30% to 50% percent of PMU coverage at typical power systems; see e.g., [24].

To demonstrate that our proposed algorithms specifically target the identification performance, we also compare with the one under the max-min error criterion in [24]. For line outage identification purpose, it is suggested in [24] to place $N_P = 9$ PMU devices at buses $\{5, 8, 9, 14, 21, 22, 24, 26, 29\}$. Under this setup, the achievable success rate is only **0.4130**, much smaller compared to **0.7028** for the BB and **0.6474** for the greedy method in our work. This speaks for the importance of directly optimizing the success rate.

Although the BB algorithm can yield the (near-) optimal solution, it is also much more computationally demanding. It is observed that the number of iterations needed for convergence is highest when N_P is in around $N/3 \sim N/2$. For example, the upper and lower bounds per iteration are plotted in Fig. 3 for placing 9 PMU devices in the 30-bus system. It takes around 4×10^4 iterations for the two bounds to approach each other, which is the largest number of iterations required among all choices of N_P in this test case. However, if one zooms in to the region of the first 500 iterations, the global optimum is actually attained at a very early stage (around 400 iterations). It takes almost all the computation time to improve the upper bound. This implies a satisfactory performance should be achieved even if the computation resource is limited and the BB algorithm has a budget on the total number of iterations.

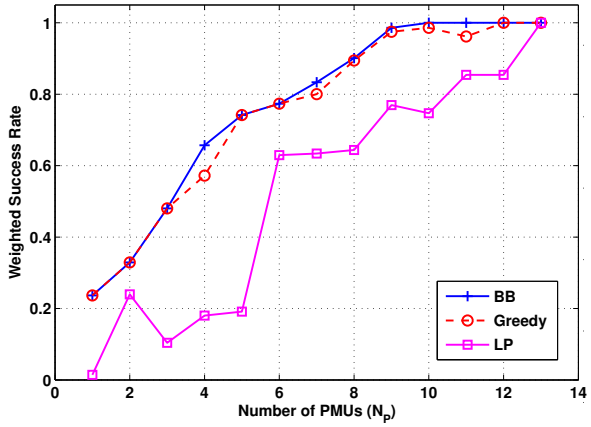

(a)

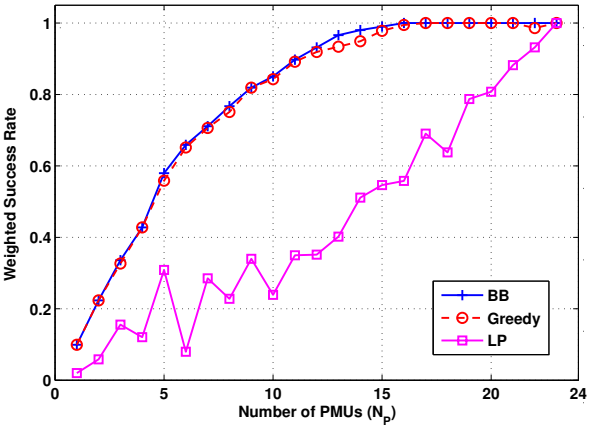

(b)

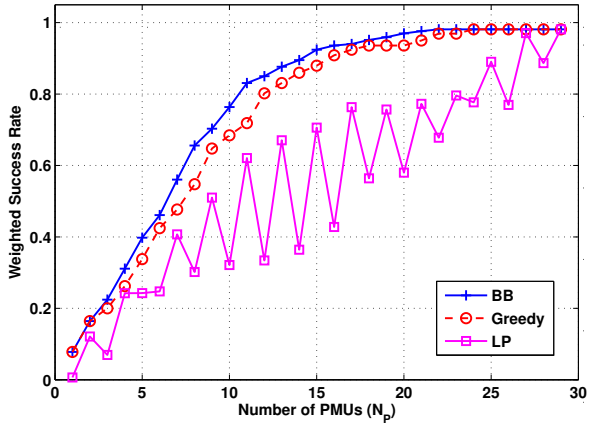

(c)

Fig. 2. The achievable detection success rate versus the number of PMU devices N_P using the LP, greedy, and BB algorithms, for (a) IEEE 14-bus system; (b) IEEE RTS 24-bus system; and (c) IEEE 30-bus system.

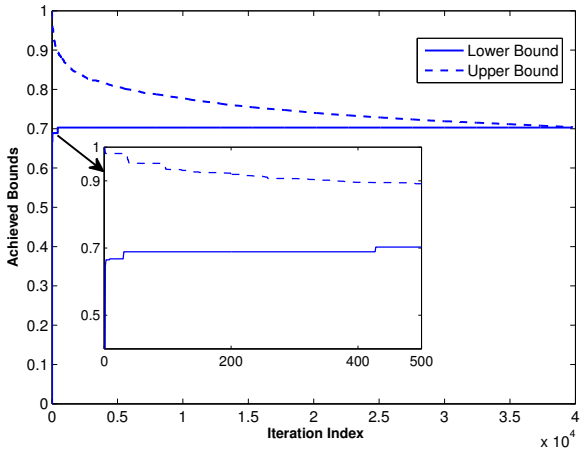

Fig. 3. The upper and lower bounds attained by the BB algorithm versus the iteration index with the 30-bus system and $N_P = 9$.

Further investigations on accelerating the BB algorithm will be an important research topic.

To test on larger systems, numerical results using the IEEE 57-bus and 118-bus cases are included. Fig. 4 plots the corresponding success rate attained by the greedy and LP methods. Similar observations also hold regarding the trade-off between the identification performance and the number of PMU devices. We plan to evaluate all proposed algorithms on more complicated test systems.

To conclude this section, we would like to report the runtime comparisons for all the test cases, as listed in Table 1. All algorithms are run using the MATLAB® R2011b software, on a Windows computer with a 3.10GHz CPU. The runtime for the LP approximation is averaged over all choices of $N_P \in [1, N]$, while the greedy method's runtime is reported for $N_P = N$ since its solutions are nested. As for the BB algorithm, the worst-case runtime is listed for the N_P value with the maximum number of iterations to converge. The greedy Algorithm 1 clearly outperforms the rest in runtime, and scales gracefully with the number of buses. The BB algorithm witnesses a dramatical increase in its runtime when the number of PMUs is in the medium range. The LP based solution is relatively fast in terms of time, but fails to be attractive in performance as shown earlier. The performance and runtime comparisons recommend the greedy method to be a competitive solution to the PMU placement problem. The BB algorithm can be used to trade-off more computational time for a near-optimal performance, especially considering that this is implemented in the planning phase and can afford a larger time scale and more demanding computational requirements.

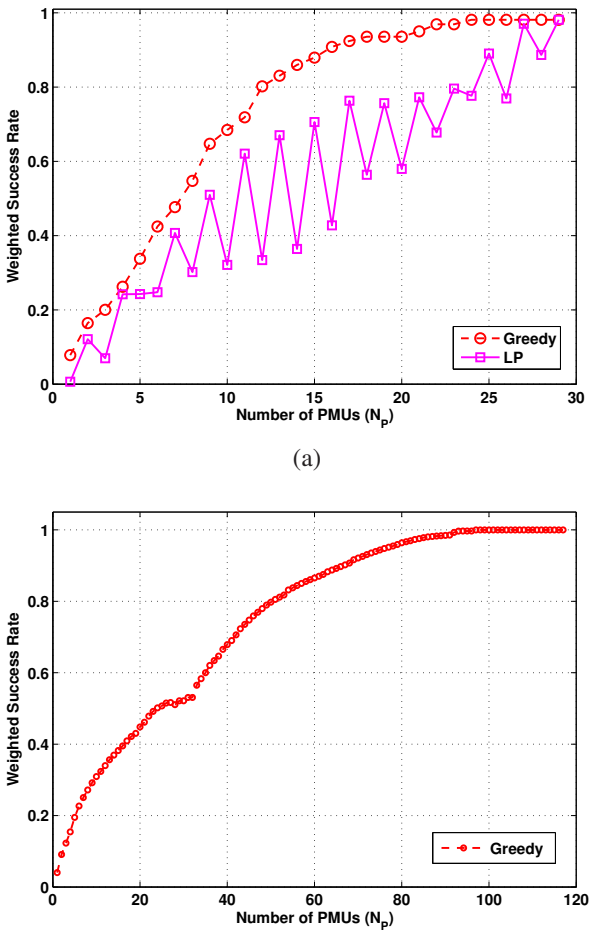

Fig. 4. The achievable detection success rate versus the number of PMU devices N_P using the LP and greedy algorithms, for (a) IEEE 57-bus system; and (b) IEEE 118-bus system.

TABLE 1. Runtime comparisons for all test cases.

	LP	Greedy	BB (worst-case N_P)
14-bus	0.25 sec	0.0015 sec	23.6 sec ($N_P = 7$)
24-bus	0.80 sec	0.0046 sec	1.5 hour ($N_P = 10$)
30-bus	1.15 sec	0.0059 sec	5.0 hour ($N_P = 9$)
57-bus	15.0 sec	0.025 sec	$\sim$
118-bus	$\sim$	0.15 sec	$\sim$

6. Discussions

6.1. Power flow model

The AC nonlinear power flow model has been used in the paper for developing the PMU placement algorithms.

Although the linearized DC power flow model is the basis to show the sparse overcomplete framework that models the multiple line outages in Section 2, it is used for neither formulating the PMU placement problem for providing the numerical results later on. The formulated problem (10) relies on the phasor angle difference vector $\mathbf{y}_\ell$ with line ℓ in outage, which is obtained from the AC flow model such as in the typical contingency analysis. The simulated tests in Section 5 also follow this setting, and thus the plotted success rate curves all correspond to the actual performance metrics under the realistic AC power flow model.

6.2. Modeling assumptions

Although some modeling assumptions have been suggested to simplify the problem formulation in Section 2, they will not significantly affect the generalizable property of the proposed problem statement and algorithms.

First, the OMP algorithm is deemed as the identification method in this paper since it achieves the best success rate as the ES method in an extremely fast fashion. Albeit optimal, the ES cannot cope with the real-time monitoring efficiency in the case of multiple line outages, because its computational time grows exponentially with the number of outage lines. The OMP method is an extremely attractive alternative to the ES, with the complexity only linear in the number of outage lines. This suggests that the PMU placement method should be developed based on the metric related to the OMP detection method, which also provides an analytical characterization for the event of successful detection.

Second, the single line outage assumption is not so limited as it seems. Extensive numerical results in [26] demonstrated that the success rate for double line outages is very close to that of single line outages. As shown in (5), the phase angel difference vector $\tilde{\boldsymbol{\theta}}$ is a linear combination of the signature vectors corresponding to the outage lines. If the related signature vectors $\{\mathbf{a}_\ell\}_{\ell\in\tilde{\mathcal{E}}}$ are almost orthogonal, then the multiple line-outage problem can just be decomposed into multiple single line-outage ones. In this sense, the weighted success rate as defined in (9) is able to capture the case of multiple line outages. The weak coupling is very likely for large-scale systems and if the number of line outages $|\tilde{\mathcal{E}}|$ is very small. This provides this intuitive explanation on the validity of the single line outage assumption.

Third, the framework in this paper can be easily generalized to multiple operating points under various load profile conditions. Suppose the number of operating points of interest is D in total. In general, the value D can be relatively small, or we can restrain to only the heavily loaded cases during which line outages are more likely to emerge. For each operating point d, the corresponding phase angle difference vector $\mathbf{y}_\ell(d)$ can be obtained per outage line ℓ, as performed routinely in power system contingency analysis. The optimization metric in (9) can be accordingly modified as

$$f(\mathcal{N}_P) := \sum_{d=1}^{D}\sum_{\ell\in\mathcal{E}} \alpha_\ell \mathbb{1}\{\mathbf{y}_{\ell,P}^T(d)\mathbf{a}_{\ell,P} \geq |\mathbf{y}_{\ell,P}^T(d)\mathbf{a}_{k,P}|\}. \tag{20}$$

This slight modification of the objective function neither complicates the problem formulation nor changes the developed algorithms. Hence, it is possible to generalize the framework of the fixed operating point to account for various loading conditions in the system, which we will leave as our future work. .

6.3. A hybrid greedy-BB method

Finally, we would like to offer a hybrid algorithm that can potentially combine the attractive complexity of the greedy method and the BB's performance optimality. As emphasized earlier, the greedy method is shown to be satisfactory numerically, but it is still not clear how to assert its performance guarantee. Since the PMU placement problem (13) is a non-convex MINLP, it is generally very hard to solve and has to rely on a specifically designed BB method. The trade-off of the BB solution is obviously the rapidly growing complexity, especially if the number of PMUs is around half of the total number of buses. This motivates us to consider to adopt the BB iterations by reducing the number of locations from N to N_G through performing the fast greedy procedure. Specifically, based on the values N and N_P we can design the input to the greedy algorithm, namely the number of PMUs $N_G \in [N_P, N]$. The purpose is to drive the ratio N_P/N_G away from $1/3 \sim 1/2$ such that there are much fewer combinations when picking N_P locations from N_G buses. With the satisfactory performance of the greedy method, it is reasonable to presume that the chosen N_G buses can capture the best N_P locations, while picking the locations from N_G buses will be more computationally efficient. This hybrid method can be thought of as using the greedy to provide a *warm start* for the BB iterations. Exploring this potential hybrid method is a very exciting future research direction.

7. Conclusions and future research

This paper presents the PMU placement problem for line outage identification, an important power system monitoring task. Using the OMP based identification algorithm, the weighted rate of correct detection is explicitly formulated as the objective for optimal PMU placement under the budget of available devices. This discrete set optimization problem is first reformulated as an LP using convex relaxation technique and an approximate objective function. The LP approximation is efficiently solvable, and provides an upper bound estimate for the optimal value of the original problem. To directly tackle the set constraint, a greedy heuristic method has been developed with the complexity growing only linearly in the number of PMU devices. Furthermore, the BB algorithm has

been adopted which can achieve a δ-optimal solution to the PMU placement problem. Numerical tests greatly advocate the greedy heuristic method, which can be very competitive to the optimal performance at a relatively affordable complexity.

Future research directions include extensive simulations for more complicated scenarios such as diverse load profiles and higher system uncertainties. It is also of great interest to further reduce the complexity for the BB algorithm to make it more attainable for large-scale systems, possibly by a more accurate upper bound estimate and the hybrid method.

References

[1] D. A. Bader, W. E. Hart, and C. A. Phillips, "Parallel algorithm design for branch and bound," *International Series in Operations Research & Management Science*, vol. 76, pp. 5-1-5-44, 2005.

[2] E. Balas, "A note on the branch-and-bound principle", *Operations Research*, vol. 16, pp. 442–445, 1968.

[3] S. Boyd and L. Vandenberghe, *Convex Optimization*, Cambridge, UK: Cambridge University Press, 2004.

[4] S. Burer and A. N. Letchford, "Non-convex mixed-integer nonlinear programming: A survey", *Surveys in Operations Research & Management Science*, vol. 17, no. 2, pp. 97–106, July 2012.

[5] E. J. Candès and T. Tao, "Near-optimal signal recovery from random projections: universal encoding strategies?," *IEEE Trans on Info. Theory*, vol. 52, pp. 5406–5425, Dec. 2006.

[6] J. Clausen and J. L. Traff, "Implementation of parallel branch-and-bound algorithms – experiences with the graph partitioning problem," *Annals of Operations Research*, vol. 33, no. 5, pp. 329-349, 1991.

[7] M. X. Goemans, N. J. A. Harvey, S. Iwata, and V. Mirrokni, "Approximating submodular functions everywhere," in *Proc. 20th ACM-SIAM Symp. on Discrete Algorithms*, pp. 535–544, 2009.

[8] M. X. Goemans and D. P. Williamson, "Improved approximation algorithms for maximum cut and satisfiability problems using semidefinite programming," *Journal of the ACM*, vol. 42, no. 6, pp. 1115–1145, 1995.

[9] T. Güler, G. Gross, and M. Liu, "Generalized line outage distribution factors," *IEEE Trans. on Power Systems*, vol. 22, no. 2, pp. 879–881, May 2007.

[10] V. Kekatos, G. B. Giannakis, and B. Wollenberg, "Optimal placement of phasor measurement units via convex relaxation," *IEEE Trans. on Power Systems*, vol. 27, no. 03, pp. 1521-1530, Aug. 2012.

[11] E. L. Lawler and D.E. Wood, "Branch-and-bound methods: A survey", *Operations Research*, vol. 14, pp. 699–719, 1966.

[12] Q. Li, T. Cui, Y. Weng, R. Negi, F. Franchetti, and M. D. Ilic, "An information-theoretic approach to PMU placement in electric power systems," *IEEE Transactions on Smart Grid*, vol. 4, no. 1, pp. 446–456, March 2013.

[13] G. L. Nemhauser , L. A. Wolsey and M. L. Fisher, "An analysis of approximations for maximizing submodular set functions", *Math. Programm.*, vol. 14, pp.265–294, 1978.

[14] A. G. Phadke and J. S. Thorp, *Synchronized Phasor Measurements and Their Applications.* New York: Springer, 2008.

[15] Power Systems Test Case Archive, *University of Washington*. [Online.] Available: http://www.ee.washington.edu/research/pstca/

[16] J. F. Sturm, "Using SeDuMi 1.02, a matlab toolbox for optimization over symmetric cones," *Optimization Methods Software*, vol. 11–12, pp. 625–653, Aug. 1999. [Online]. Available: http://sedumi.mcmaster.ca

[17] J. E. Tate and T. J. Overbye, "Line outage detection using phasor angle measurements," *IEEE Trans. on Power Sys.*, vol. 23, no. 4, pp. 1644–1652, Nov. 2008.

[18] J. E. Tate and T. J. Overbye, "Double line outage detection using phasor angle measurements," in *Proc. of IEEE PES General Meeting*, Calgary, AB, July 26–30, 2009.

[19] V. Terzija, G. Valverde, D. Cai, P. Regulski, V. Madani, J. Fitch, S. Skok, M. Begovic, and A. Phadke, "Wide-area monitoring, protection and control of future electric power networks," *Proc. of the IEEE*, vol. 99, no. 1, pp. 80-93, Jan. 2011.

[20] J. A. Tropp, "Greed is good: Algorithmic results for sparse approximation," *IEEE Trans. on Info. Theory*, vol. 50, no. 10, pp. 2231–2242, Oct. 2004.

[21] U.S.-Canada Power System Outage Task Force, "Final report on the August 14th blackout in the United States and Canada," Apr. 2004. [Online.] Available: https://reports.energy.gov/

[22] U.S.-Canada Power System Outage Task Force, "Final Report on the implementation of the task force recommendation," Sep. 2006. [Online.] Available: http://nrcan.gc.ca/eneene/pdf/outpan-eng.pdf

[23] A. J. Wood and B. F. Wollenberg, *Power Generation, Operation, and Control*, 2nd ed., New York, NY: John Wiley and Sons, 1996.

[24] Y. Zhao, A. Goldsmith, and H. V. Poor, "On PMU location selection for line outage detection in wide-area transmission networks," in *Proc. IEEE Power and Energy Society General Meeting*, July 22-26, 2012.

[25] R. D. Zimmerman, C. E. Murillo-Sanchez, and R. J. Thomas, "Matpower: steady-state operations, planning and analysis tools for power systems research and education," *IEEE Trans. on Power Systems*, vol. 26, no. 1, pp. 12–19, Feb. 2011.

[26] H. Zhu and G. B. Giannakis, "Sparse overcomplete representations for efficient identification of power line outages," *IEEE Trans. Power Systems*, vol. 27, no. 4, pp. 2215-2224, Nov. 2012.